Steel and Composite Structures, Vol. 4, No. 2 (2004) 149-167
DOI: http://dx.doi.org/10.12989/scs.2004.4.2.149

Reserve capacity of fatigue damaged internally ring stiffened tubular joints

T. S. Thandavamoorthy†

Shock and Vibration Laboratory, Structural Engineering Research Centre, CSIR Campus, Taramani, Chennai 600 113, Tamil Nadu, India

(Received August 5, 2003, Accepted April 7, 2004)

Abstract. Offshore platforms have to serve in harsh environments and hence are likely to be damaged due to wave induced fatigue and environmental corrosion. Welded tubular joints in offshore platforms are most vulnerable to fatigue damage. Such damages endanger the integrity of the structure. Therefore it is all the more essential to assess the capacity of damaged structure from the point of view of its safety. Eight internally ring stiffened fatigue damaged tubular joints with nominal chord and brace diameter of 324 mm and 219 mm respectively and thickness 12 mm and 8 mm respectively were tested under axial brace compression loading to evaluate the reserve capacity of the joints. These joints had earlier been tested under fatigue loading under corrosive environments of synthetic sea water and hence they have been cracked. The extent of the damage varied from 35 to 50 per cent. One stiffened joint was also tested under axial brace tension loading. The residual strength of fatigue damaged stiffened joint tested under tension loading was observed to be less than one fourth of that tested under compression loading. It was observed in this experimental investigation that in the damaged condition, the joints possessed an in-built load-transfer mechanism. A bi-linear stress-strain model was developed in this investigation to predict the reserve capacity of the joint. This model considered the strain hardening effect. Close agreement was observed between the experimental and predicted results. The paper presents in detail the experimental investigation and the development of the analytical model to predict the reserve capacity of internally ring stiffened joints.

Key words: offshore platforms; internally ring stiffened joins; cracked; reserve capacity; experimental; analytical; bi-linear constitutive model.

1. Introduction

Let us now briefly look at the extent of the energy challenge facing us. Forecasters agree that world energy demand will continue to grow for the foreseeable future. OPEC's World Energy Model projects growth of around two percent a year up to 2020, with demand in developing countries rising at three-to-four times the rate of the industrialised countries. In absolute numbers, world commercial energy demand is forecast to rise from close to nine billion tonnes of oil equivalent (toe) in 2000 to more than 13 bn toe in 2020. Ninety-five per cent of the additional demand is expected to be met by fossil fuels, which will account for 91 percent of demand in 2020 (Calderon 2003).

The efficient design of offshore hydrocarbon (oil and gas) facilities is dependent on a number of factors: geographic location, metocean data, platform configuration, expected economic return on the

†Deputy Director and Head

initial investment, the accepted probability of failure and manning status, being among the most important (Pinna *et al*. 2003).

Offshore platforms are large steel tubular framed structures installed on the sea bed for the exploration and production of oil from the sea bottom. They serve as artificial bases supporting drilling and production facilities above the elevation of waves. While a variety of platforms have been utilised offshore for exploration and production, the most popular structure for shallow water depth of upto 200 m is the jacket or 'template' platform. For offshore structures, which are subjected to fatigue by wave loading, circular hollow sections or tubular numbers are used almost exclusively due to their relatively smaller hydrodynamic loads and stress concentration in joints (Bian and Lim 2003). In the past four decades thousands of large tubular structures have been built for offshore oil drilling and production. At present there are over 7000 offshore structures worldwide (Valdés and Ramirez 2000).

The typical jacket structure consists of a deck, a substructure, and foundation piles. The substructure is a prefabricated tubular space frame, which extends from the sea floor to just above the sea surface, and is usually fabricated in one piece onshore, transported by barge, launched at sea, and upended on site by partial flooding. Tubular pilings are driven through the main legs to fix the structure to the sea bottom, provide support for the deck, and resist the lateral loadings due to wind, waves, and currents (Thandavamoorthy 2002a).

In the tubular frame, the intersection between two or more members is called a tubular connection. A welded joint at the interface created between members in a tubular connection is called a tubular joint. The main member is denoted as chord and the secondary member as brace or branch. In tubular joints, the hollow section members are joined together by welding the profiled ends of secondary members, the braces, due to their complicated joint geometry. A joint without reinforcements of any sort is called an unstiffened joint. This kind of joint requires no additional connecting elements, makes materials savings, and is with high load-bearing capacity. Because of these merits, there has been an ever increasing use of this joint type in offshore structures (Chen and Wang 2003). Also, the behaviour of these welded tubular connections, even in their simplest configuration, is complex and their analysis is difficult (Bian and Lim 2003).

Since 1950, researchers have carried out a large amount of experimental and theoretical analyses on the structural behaviour of unstiffened tubular joints. Most of this research focused on issues such as the determination of static strength, the evaluation of stress concentration factors and also the fatigue behaviour (UEG 1985 a, b and c). A new static strength numerical database of some 320 planar and multiplanar tubular joints under axial load cases has been generated (Dexter and Lee 2001). Main research achievements have been introduced into designing specifications or handbooks. According to Choo *et al*. (2003), the strength formulations in design codes were developed using joint databases, which have been established by international researchers over the last few decades.

The joints must be properly dimensioned during the design stage so that they perform satisfactorily in service and achieve a reasonable balance between economy and risk of failure. The basic design requirements of joints are that they must possess adequate static strength and satisfy fatigue endurance requirements (UEG 1985a). If the capacity of a joint is found to be inadequate during the design stage, it can be enhanced by introducing stiffeners to the inside of the chord as this is an efficient method to reduce stress concentration, increase load carrying capacity and fatigue life of joint (Bozhen 1990), decrease the bending stress in tube walls and avoid attraction of additional wave forces. These types of joints are called internally ring stiffened joints (Thandavamoorthy 2002b).

Offshore structures have to serve in harsh environments and are exposed to extreme conditions of the environment such as wave slam, ice impact, and fatigue. They are also subjected to environmental corrosion which weakens the structure beyond allowable limits. Wave induced fatigue coupled with environmental corrosion can cause extensive damage to offshore platforms. Ocean waves, loading a tubular structure, cause fluctuations in the stress levels at the joints. The fatigue performance of a joint is known to be influenced by the local stress concentrations due to weld geometry and irregularities at the weld toe (Van Wingerde *et al*. 1996). Due to the cyclic nature of loading and weld effects, high stress concentrations are induced around joint intersection at critical locations (Gowda 1991), leading to fatigue crack growth and eventual failure. Fatigue failure invariably occurs at the joints because of the concurrence of a number of features which lead to poor fatigue performance. The accurate prediction of the structural integrity of such structures requires consideration of the effect of both part and through-thickness cracks on the static strength of tubular joints (Saad *et al*. 2001).

In the event of the occurrence of damage to the fixed offshore structures, it is all the more essential that the damage is properly assessed and the member or joint is properly rehabilitated in order to ensure the safety of the structure so that it may continue to serve its intended functions for the specified design life. While a number of investigations have been carried out on the assessment of the reserve capacity of dent and bend damaged simple tubular members (Thandavamoorthy *et al*. 1995a, 1995b, Thandavamoorthy *et al*. 1998), information on the estimation of the reserve strength of corrosion fatigue damaged tubular joints are scarce. Lie *et al*. (2001) have described a new modelling procedures for the geometrical modelling, finite element mesh generation and estimation of stress intensity factors of unstiffened T and Y joint containing through thickness or surface cracks. It enables cracks of any length to be located at any point along the intersection between the weld toe and the chord member. This is particularly significant as it is found in practice that the initiation site of a surface crack does not always start from the saddle or crown position when these tubular joints are subjected to a combination of axial, in-plane, and out-of-plane loading. One typical T-joint containing a surface semi-elliptical crack at the saddle position has been analysed using this new modelling approach, and the results were used to evaluate the stress intensity factor (SIF) of the crack. The SIF validation results demonstrate that the model is reliable.

The results of ultimate strength investigations on cracked tubular K joints subject to balanced axial brace loading have been reported (Cheaitani and Burdekin 1994). These studies involve using both the non-linear finite element technique and a series of small scale experimental tests on twelve joints at room and low temperature on joints in both the uncracked and the through thickness cracked conditions. The small scale tests have confirmed and agreed reasonably well with the findings of the finite element analyses. The chord diameter in these experiments varied from 76.2 mm to 168.4 mm and thickness from 3.2 to 6.0 mm. The brace diameter was 60.4 mm and thickness varied from 3.2 mm to 4.9 mm.

A finite element study on the effect of crack extent on the static strength of a tubular T-joint under the axial tensile loading has been carried out by Saad *et al*. (2001) Comparisons were made with published experimental test results for a range of crack angles. Both the finite element and experimental results show that the strength reduction is approximately linearly dependent on the crack angle and the ratio of crack depth to thickness. While a lot of investigations have been carried out to determine the strength of cracked unstiffened tubular joints, little is known on the evaluation of residual strength of the fatigue damaged internally ring stiffened tubular joints. Moreover, most of the theoretical investigations concerning the prediction of strength of cracked unstiffened joints have mainly focussed on the finite element studies which have their own problems in modelling the weld and the crack profile, and many times the correlation between experimental and numerical values were found to be not so satisfactory. Also, with the presence of crack, the joint becomes unsymmetrical and hence modelling based on symmetry is no more valid. Development of mathematical model for the prediction of strength is scanty. Therefore, there is a need to develop a methodology to assess the residual strength of the damaged tubular joints as such. This methodology has to be validated with experimental results. Towards this goal, experimental and analytical investigations were carried out to determine the reserve capacities of cracked internally ring stiffened tubular T and Y joints (Thandavamoorthy 1998).

The paper presents a complete description of the experimental investigation carried out on fatigue cracked internally ring stiffened joints and the development of an analytical model to predict the reserve capacity of stiffened joints.

2. Experimental investigation

The geometrical configuration of a typical internally ring stiffened damaged T joint is shown in Fig. 1a

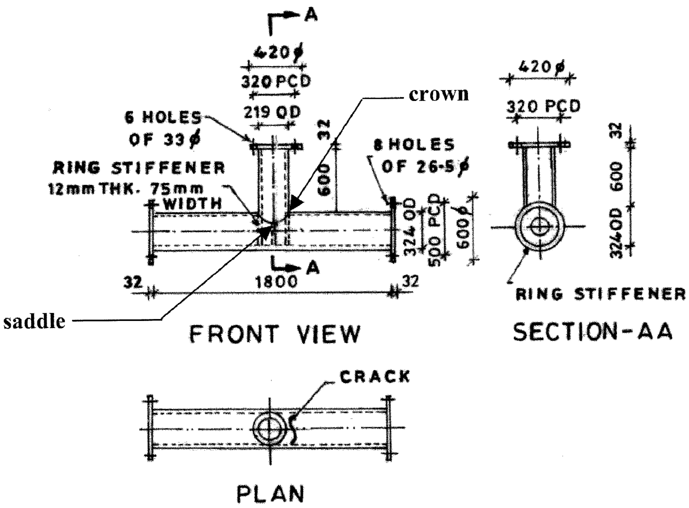

(a) Cracked T-joint

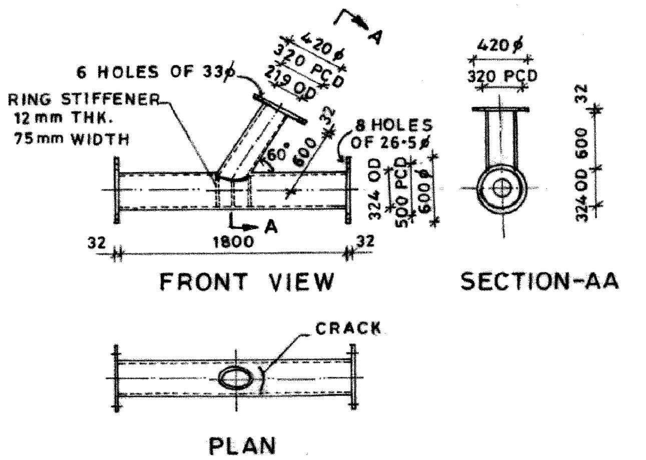

(b) Cracked Y-joint

Fig. 1 Typical cracked welded joints

Table 1 Dimensions of the damaged stiffened tubular T and Y joints

S. No.	Specimen No.	Dimensions of the joint (mm)				Length of the crack (mm)
		Chord		Brace		
		Diameter	Thickness[a]	Diameter	Thickness[a]	
1	DT1[b]	320.00	12.00	219.00	8.00	365.00
2	DT2[b]	316.72	12.00	221.54	8.00	346.00
3	DT3[b]	320.54	12.00	218.68	8.00	455.00
4	DY1[b]	319.86	12.00	220.50	8.00	405.00
5	DY2[c]	320.27	12.00	221.23	8.00	395.00
6	DY3[b]	321.27	12.00	219.80	8.00	431.00
7	DY4[c]	320.68	12.00	220.00	8.00	422.00
8	DY5[b]	321.10	12.00	219.50	8.00	493.00

a-Nominal Values; b-IS: 226 Steel; c-AP15L GB Steel

and a Y joint in Fig. 1b. The dimensions of joints, such as outside diameter and thickness of the chord and brace members of the T and Y joints are given in Table 1. These joints have been tested earlier under fatigue loading under corrosive environments of sea water, synthesized according to the ASTM Standards D 1141 (ASTM 1980). Due to the synergetic action of fatigue and corrosion, these joints have developed through thickness crack along the circumference of the chord member. Because of the aggressive environment, corrosion patches have been formed on the immersed portion of the chord member. The length of the circumferential crack for each joint was measured. The crack lengths in respect of T and Y joints are given in Table 1. The extent of the damage varied from 35 to 50 percent. The material quality of the joint was in conformity with API5L GB (API RP2A 1993) and IS: 226 (IS 226, 1975) with the yield strength of 240 MPa and ultimate tensile strength 415 MPa. In all, three fatigue damaged ring stiffened T joints and five fatigue damaged ring stiffened Y joints were tested.

Joints were fixed to the steel pedestals by bolting. The pedestals in turn were fixed to the strong concrete floor by means of MS bolts of 60 mm size. The entire assembly was placed under a reaction frame (Fig. 2). On the flange of the brace member, and between the horizontal cross beam of the reaction frame and the flange, a 2000 kN hydraulic jack and a proving ring were placed as shown in Fig. 2. The jack was connected to the electrically operated pumping unit by means of high pressure rubber hoses. Three dial gauges, reading to 0.01 mm, were mounted beneath the joint, one directly under the load point and the other two approximately at the third points, to facilitate recording of the deflection readings under load. Axial brace loading in compression was applied on the joints by means of the hydraulic jack. Load was applied in equal increments. For each load increment, deflection readings of all the gauges were recorded. Load was monotonically increased till the ultimate load was reached.

A typical load-midspan relation for fatigue damaged T joint, tested under monotonic axial brace loading, is shown in Fig. 3. It has been observed that initial yielding occurs first at the cracked section (Fig. 3). The observed load corresponding to the initial yielding of the cracked section for various joints are given in Table 2. The uncracked full cross section yielded later. Load corresponding to the yielding of the full cross section is given in Table 2 for each tested joint. In the case of Y joint, the relation for the load-midspan deflection is shown in Fig. 4. It has been observed from the load-deflection behaviours of these damaged joints that they display strain-hardening characteristics (Figs. 3 and 4). The ultimate loads measured in the experimental investigation for different tested joints are given in Table 2.

Fig. 2 Typical test set-up for axial brace compression loading

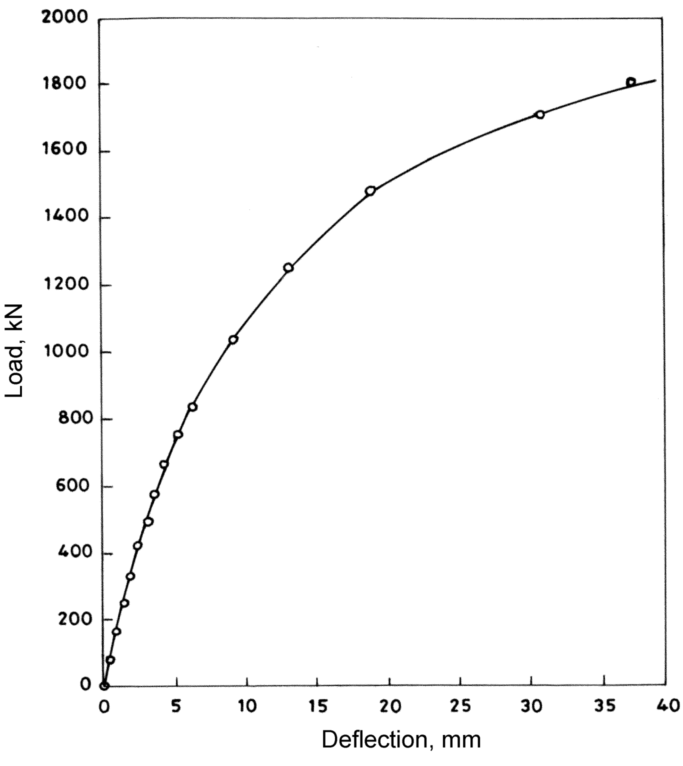

Fig. 3 Typical load-midspan deflection for damaged T joint

Table 2 Measured and predicted results of damaged joints

S. No.	Specimen No.	Strength at yielding of cracked section (kN)		Strength at yielding of full section (kN)		Ultimate Strength (kN)	
		Exptl.[2]	Analytl.	Exptl.[2]	Analytl.	Exptl.	Analytl.
1	DT1	300.00	366.65	700.00	953.68	900.00[1]	1819.28
2	DT2	415.10	406.80	850.00	957.02	1822.70	1780.74
3	DT3	350.00	297.51	850.00	957.02	1740.90	1825.66
4	DY1	500.00	374.97	1040.00	952.81	1859.10	1817.62
5	DY2	330.00	395.18	750.00	955.35	1677.30	1822.47
6	DY3	415.10	334.92	740.00	961.56	1600.00	1834.31
7	DY4	415.10	345.48	1000.00	957.90	1759.10	1827.32
8	DY5	250.00	244.25	840.00	960.50	1781.80	1832.30

Note: [1]- Limited due to the lower capacity of the actuator
[2]- Extracted from the load-deflection curve of appropriate joint

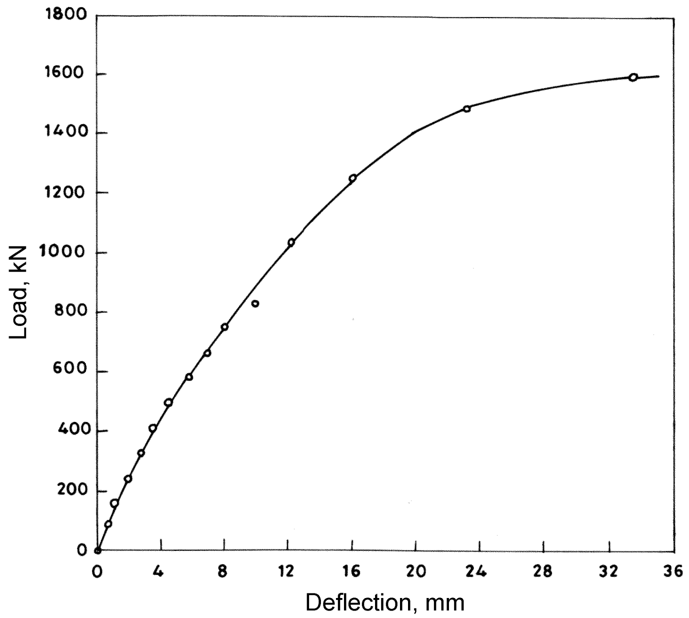

Fig. 4 Typical load-midspan deflection curve for damaged Y joint

Joint DT1 alone was also tested under axial brace tension loading using Instron servo-hydraulic dynamic testing system (Fig. 5) to assess the strength of this cracked joint under this type of loading. As before, load on the joint was applied in increments. For each load increment, the mid-span deflection was measured by a dial gauge mounted underneath the chord member. The width of the pre-existing crack started increasing at the load of 40 kN. At the load of 160 kN, the crack started propagating along the circumference. At 400 kN, the brace was severed from the chord by fracturing of the weld. The load-midspan deflection relation for this tension loading is shown in Fig. 6.

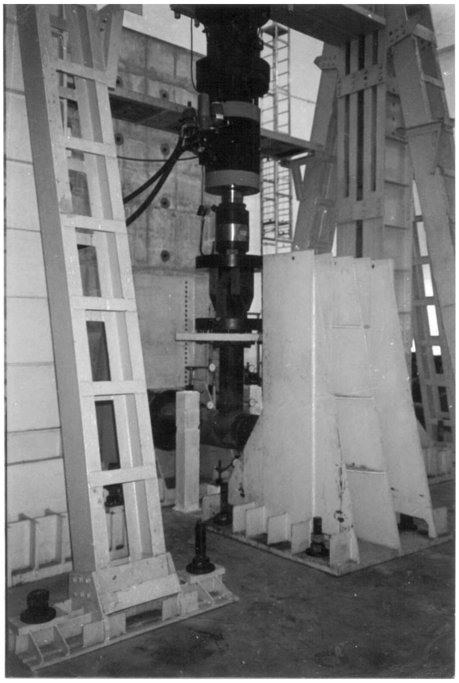

Fig. 5 Typical test set-up for axial brace tension loading

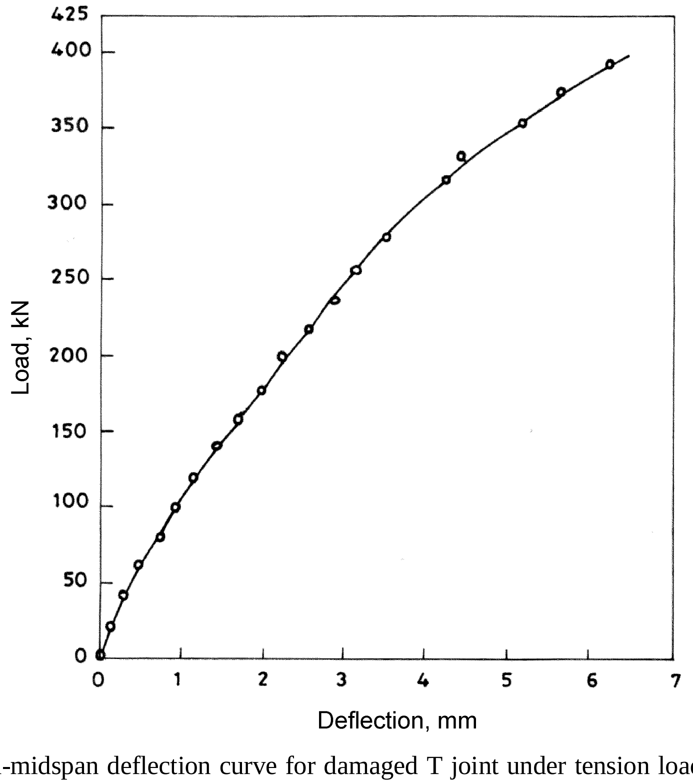

Fig. 6 Load-midspan deflection curve for damaged T joint under tension loading-typical

3. Development of an analytical model

3.1. Cracked section strength

An analytical model was developed to assess the strength of the internally ring stiffened fatigue damaged joints. As stated before, the experimental load-deflection relation of the typical tested T joint (Fig. 3) clearly displays the strain hardening characteristics of the material of the joint. The conventional linear elastic-perfectly plastic model, therefore, cannot be a suitable proposition for this type of behaviour. Therefore the strain hardening property was taken into consideration in modelling the joint. According to the proposed model, linear elastic behaviour upto the yield was assumed. After yielding, linear strain hardening behaviour upto the ultimate strength was considered. This model is illustrated in Fig. 7. The strain energy represented by the area under the stress-strain curve of the proposed model (Fig. 7) was computed and was compared with the work done of the joint represented by the area under the load-deflection curve of a typical T joint (Fig. 3) and was found that both the values were equal.

Based on this proposed model, the moment capacity of the fatigue damaged internally ring stiffened tubular joints was derived from the first principles. As the joints had developed circumferential and through thickness cracks, the area of the cross section of the joint has been reduced to some extent and the resulting effective section is shown in Fig. 8. Due to cracking, the cross section has become unsymmetrical. So the C.G. of the section was shifted from its original position by a quantity e_d. It was

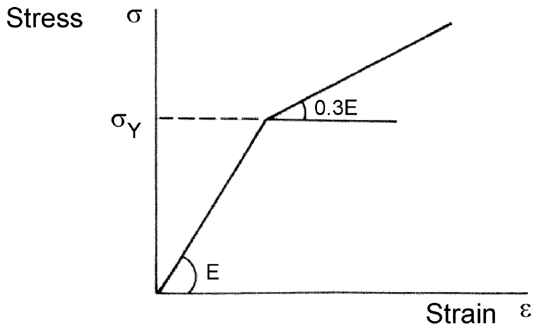

Fig. 7 Proposed analytical model

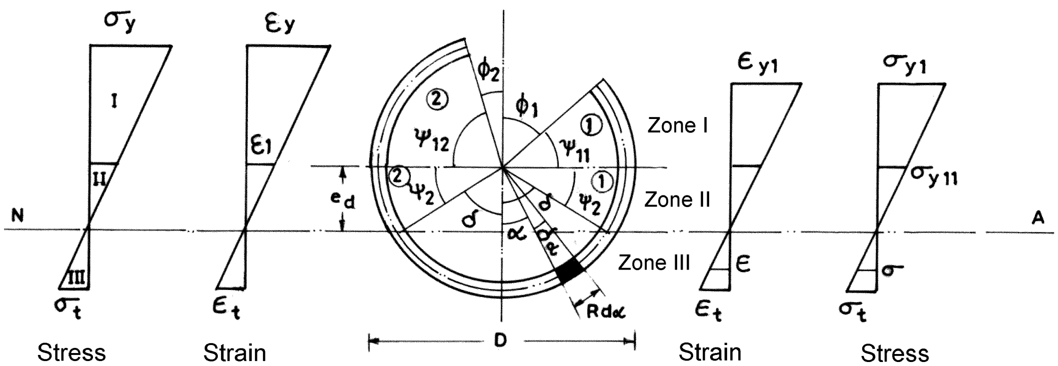

Fig. 8 Strain and stress distributions across a cracked section

observed during testing of damaged joint that the cracked section yielded first. Then a redistribution of loads took place. As a result of this, the uncracked full cross section at mid-span yielded next. After this, strain hardening occurred and the behaviour became non-linear as is evident from Fig. 3. In consonance with this observation, it is assumed that the extreme fibre on the compression side of the cracked section yields first. As the joint had already been subjected to fatigue loading and as consequence of this it had been cracked, there is a possibility that the yield strength of the steel would have increased beyond 240 MPa. Therefore, a higher value of the yield strength, even upto ultimate strength depending upon the extent of cracking, was assumed in the assessment of the residual strength of the damaged joints.

The strain and stress distributions across the cracked section is shown in Fig. 8. The stress distribution is linear because of initial yielding. For this particular distribution of stresses, forces in various segments were computed. The depth of the neutral axis e_d, from the centre of the circle, was determined by considering the equilibrium of forces by iterative technique. The value of the neutral axis, e_d, thus determined, was used to compute the moments in various segments.

The angle ϕ_1 of segment 1 of zone I and angle ϕ_2 of segment 2 of zone I corresponding to the cracked lengths are calculated first. From the known values of these two angles, ϕ_1 and ϕ_2, angles ψ_{11} and ψ_{12} corresponding to the compression area in zone I are determined. For a known value of e_d, angle ψ_2 in zone II is given in Eq. (1) and angle δ of zone III in Eq. (2):

$$\psi_2 = \sin^{-1}\left(\frac{e_d}{R}\right) \tag{1}$$

$$\delta = 90^0 - \psi_2 \tag{2}$$

For the derivation of the forces in different segments, an elemental area $d\alpha$ was considered at an angle α from the appropriate axis. The compressive force in segment 1 of zone I above the neutral axis is given in Eq. (3):

$$F_{c11} = Rt\left\{\sigma_{y11}\psi_{11} + \frac{(\sigma_{y1} - \sigma_{y11})}{\cos\phi_1}(1 - \sin\phi_1)\right\} \tag{3}$$

where

$$\sigma_{y1} = \frac{\sigma_y}{\left(\cos\phi_2 + \dfrac{e_d}{R}\right)}\left(\cos\phi_1 + \frac{e_d}{R}\right) \tag{4}$$

and

$$\sigma_{y11} = \frac{\sigma_{y1}}{\left(\cos\phi_1 + \dfrac{e_d}{R}\right)}\left(\frac{e_d}{R}\right) \tag{5}$$

where σ_y is the yield strength of the steel.

The compressive force in segment 2 of zone I above the neutral axis is given in Eq. (6):

$$F_{c12} = Rt\left\{\sigma_{y11}\psi_{y12} + \frac{(\sigma_y - \sigma_{y11})}{\cos\phi_2}(1 - \sin\phi_2)\right\} \tag{6}$$

The compressive force in zone II is given in Eq. (7):

$$F_{c2} = \frac{2Rt\sigma_{y11}}{\sin\psi_2}(\psi_2 \sin\psi_2 + \cos\psi_2 - 1) \tag{7}$$

The total compression is given by Eq. (8):

$$F_c = F_{C11} + F_{C12} + F_{C2} \tag{8}$$

The tensile force in the zone Ill below the neutral axis is given in Eq. (9):

$$F_t = \frac{2Rt\sigma_t}{(1-\cos\delta)}(\sin\delta - \delta\cos\delta) \tag{9}$$

The moment of resistance of the cracked section was derived by taking moment of all the above forces about the neutral axis. The moment of the compressive force in segment 1 of zone I is given in Eq. (10):

$$M_{C11} = R^2 t \begin{bmatrix} \sigma_{y11}\left\{1 - \sin\phi_1 + \dfrac{e_d}{R}\psi_{11}\right\} + \dfrac{1}{4}\dfrac{(\sigma_{y1} - \sigma_{y11})}{\cos\phi_1} \\ \left\{2\psi_{11} - \sin 2\phi_1 + \dfrac{4e_d}{R}(1 - \sin\phi_1)\right\} \end{bmatrix} \tag{10}$$

The moment of the compressive force in segment 2 of zone I is given in Eq. (11):

$$M_{C12} = R^2 t \begin{bmatrix} \sigma_{y11}\left\{1 - \sin\phi_2 + \dfrac{e_d}{R}\psi_{12}\right\} + \dfrac{1}{4}\dfrac{(\sigma_{y1} - \sigma_{y11})}{\cos\phi_2} \\ \left\{2\psi_{12} - \sin 2\phi_2 + \dfrac{4e_d}{R}(1 - \sin\phi_2)\right\} \end{bmatrix} \tag{11}$$

The moment of the compressive force in zone II is given in Eq. (12):

$$M_{C2} = \frac{2R^2 t\sigma_{y11}}{\sin\psi_2}\left\{\begin{array}{l} \sin\psi_2\left(\dfrac{e_d}{R}\psi_2 + \cos\psi_2 - 1\right) + \\ \dfrac{e_d}{R}(\cos\psi_2 - 1) + \dfrac{1}{4}(2\psi_2 - \sin 2\psi_2) \end{array}\right\} \tag{12}$$

The moment of the tensile force in zone III is given in Eq. (13):

$$M_t = \frac{2R^2 t\sigma_t}{(1-\cos\delta)}\left[\frac{1}{4}(2\delta - \sin 2\delta) - \frac{e_d}{R}(\sin\delta - \delta\cos\delta)\right] \tag{13}$$

The total moment of resistance of the cracked section is given in Eq. (14)

$$M = M_{C11} + M_{C12} + M_{C2} + M_t \tag{14}$$

3.2. Exclusively cracked section

When cracking is extensive and the angle ϕ_1 in segment 1 of zone I is greater than 90°, the stress distribution for this case is illustrated in Fig. 9. As before, the area of the cross section corresponding to the compressive force in segment 1 of zone I is not available in this case. The area of cross section for the compression in zone II above the neutral axis also gets modified as shown in Fig. 9 in contrast to that shown in Fig. 8 for the case of less cracked section. Therefore, Eq. (3) cannot be used in this case. The compressive force in segment 1 of zone II is given by Eq. (15):

$$F_{C21} = \frac{Rt\sigma_{y1}}{\left(\frac{e_d}{R} - \sin\psi_{11}\right)}\left[\frac{e_d}{R}\psi_{21} + \cos(\psi_{21} + \psi_{11}) - \cos\psi_{11}\right] \tag{15}$$

The compressive force in segment 2 of zone II is given by Eq. (16):

$$F_{C22} = (1/2)\, F_{C2} \tag{16}$$

In this case the total compressive force is given by Eq. (17) as against Eq. (8) given above for the case of less cracked section:

$$F_c = F_{C12} + F_{C21} + F_{C22} \tag{17}$$

The moment of resistance of the cracked section in which the cracking is extensive with the result the compression area in segment 1 of zone I not being available and segment I of zone II correspondingly being reduced is given in Eq. (18) as against that given by Eq. (10) given above for the other case:

$$M_{C21} = \frac{R^2 t\sigma_{y1}}{\left(\frac{e_d}{R} - \sin\psi_{11}\right)}\left\{\begin{matrix}\left(\frac{e_d}{R}\right)^2\psi_{21} + 2\frac{e_d}{R}(\cos\overline{\psi_{11} + \psi_{21}} - \cos\psi_{11}) + \\ \frac{1}{4}(2\psi_{21} - \sin 2\overline{\psi_{11} + \psi_{21}} - \sin 2\psi_{11})\end{matrix}\right\} \tag{18}$$

The moment of the compressive force in segment 2 of zone II is obtained from Eq. (12) and is given as

$$M_{C22} = (1/2)\, M_{C2} \tag{19}$$

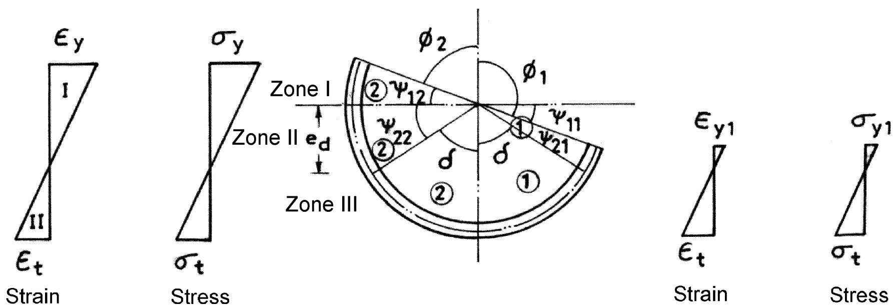

Fig. 9 Strain and stress distributions of an extensively cracked section

The moment of resistance of the extensively cracked section, with the absence of compression area in segment 1 of zone I and with the reduced area of segment 1 of zone II is given in Eq. (20).

$$M = M_{C12} + M_{C21} + M_{C22} + M_t \tag{20}$$

As the procedure for the calculation of forces involves iteration and laborious too, a computer programme in FORTRAN language was developed for the computation of the forces. With an assumed initial value of e_d, different forces were calculated. Total compression was equated to the total tension. Equilibrium was checked. If equilibrium was not satisfied, then the calculations were repeated with another value of e_d. The iteration stops when the compression and total tension are equal and the force equilibrium was achieved. The value of e_d corresponding to the force equilibrium was used to compute various moments. All the individual moments were added up to arrive at the final moment of resistance of the cracked section.

3.3. Strength of uncracked full section at initial yielding

The strain and stress distributions for an uncracked full cross section is shown in Fig. 10. As the cross section is symmetrical, the C.G. lies at the centre of the circle. In this case, the areas of the compression and tension are equal and hence the forces are in equilibrium because the stresses are also equal. Therefore, moments of forces about the C.G. are calculated directly. An elemental area $d\alpha$ of at angle α about the vertical axis is considered for the derivation of the moment. The moment of resistance of the full section at initial yielding is given as

$$M = \pi R^2 t \sigma_y \tag{21}$$

3.4. Strength of full section considering strain hardening effect

The strain and stress distributions for the ultimate strength of the full section in a cracked joint, considering the strain hardening effect, are shown in Fig. 11. The moments of the different forces about the C.G. are taken as the section and the stresses are symmetrical. The moment of forces in zone I is given as

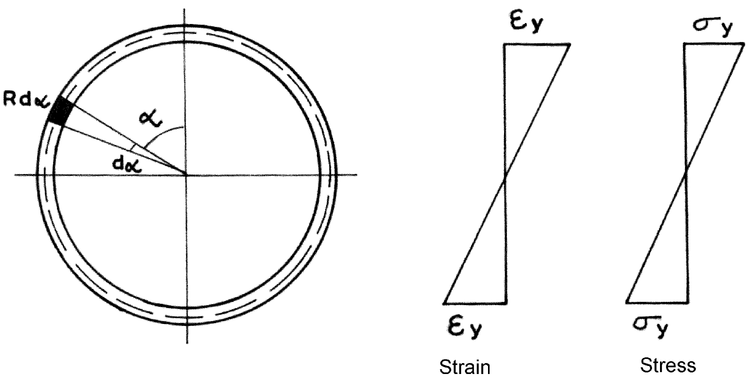

Fig. 10 Strain and stress distributions of an uncracked section at initial yielding

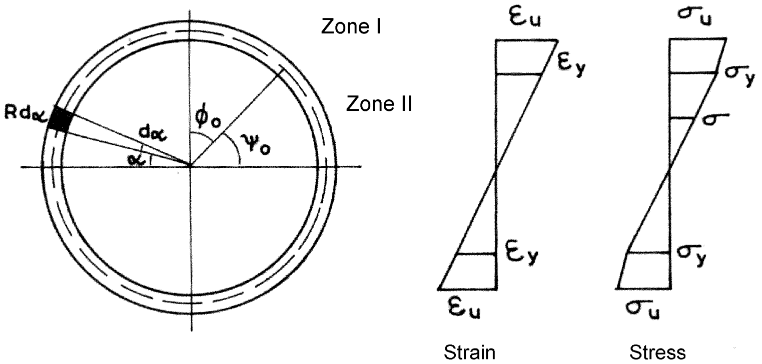

Fig. 11 Strain and stress distributions of an uncracked section at ultimate load

$$M_I = 4R^2t\left\{\sigma_y\sin\phi_o + \frac{1}{4}\frac{(\sigma_u-\sigma_y)}{(1-\cos\phi_o)}[2\phi_o - \sin 2\phi_o]\right\} \tag{22}$$

The moment of forces in zone II is given as

$$M_{II} = \left\{\sigma_y R^2 t\left[\frac{(2\psi_o - \sin 2\psi_o)}{\sin 2\psi_o}\right]\right\} \tag{23}$$

The moment of resistance of the section is given by:

$$M = M_I + M_{II} \tag{24}$$

The moment capacity of the uncracked section derived above was also included in the computer programme developed for cracked section to make it a full pledged programme.

4. Discussion of test results

The conventional procedure for the design and analysis of offshore structures assume that the joints are completely rigid. In other words, it is supposed that no local distortion of the chords in circular cross-section occurs and hence there are no tilt, compressive or tensile deformation in the direction of brace members within the joint zone of chord member. As a matter of fact, most unstiffened tubular joints are not completely rigid and the loaded braces always cause local distortion of the chord cross-section. (Chen and Wang 2003). The author has also observed during testing of unstiffened tubular joints that ovaling of chord member occurred under axial brace compression loading and at ultimate load the brace punched into the chord (Thandavamoorthy 2003).

In contrast to this, it was observed in the present experimental investigations that the predominant mode of deformation in the case of all tested internally ring stiffened damaged T joints was bending of the chord member as a whole. Absolutely no ovaling and consequent punching of chord occurred in the vicinity of the welded intersection.

The load computed, based on the analytical model developed for the initial yielding of the cracked section along with the measured values are given in Table 2. Similarly load at the initial yielding and at ultimate stage of the full cross section, both measured and calculated based on the proposed analytical model are also given in Table 2. In the case of joint DT1, it was not possible to go upto the ultimate load because the loading system has the capacity to load upto 900 kN only. Since the brace of joint DY3 was slightly tilted, load could not be continued beyond 1600 kN. In the case of joint DY4 during test, the crack widened and one portion of the crack pierced through the other half. Therefore, test was terminated at a load of 1759.10 kN. On the whole, the predicted loads in all the cases are in reasonable agreement with the measured values.

The distinct advantage of the ring stiffened tubular joint was clearly visible in this experimental investigation in that, as soon as the cracked section was yielded, a redistribution of load occurred and the uncracked full section was able to carry on the load till the ultimate stage. This could be possible only because of the flexural bending of the chord member. This could not have been possible in the case of unstiffened joint which normally would have failed by ovaling and punching and could not have taken further load because local punching and ovaling of the chord wall cannot transfer load to the adjoining uncracked section.

During the test, it was observed that in joints DT2 and DY1, due to the stiffener being welded away from the brace face, the chord wall between the stiffener and the brace face deflected near ultimate load, perhaps affecting the load carrying capacity of the joints to some extent. However, no ovaling of chord member occurred. This brings out to the fore the influence of improper fabrication methods which defeats the purpose for which the stiffeners have been welded to the chord wall. In the case of joint DY4, at the cracked section, one part of the chord wall in the compression side pierced through the other part telescopically at the ultimate load.

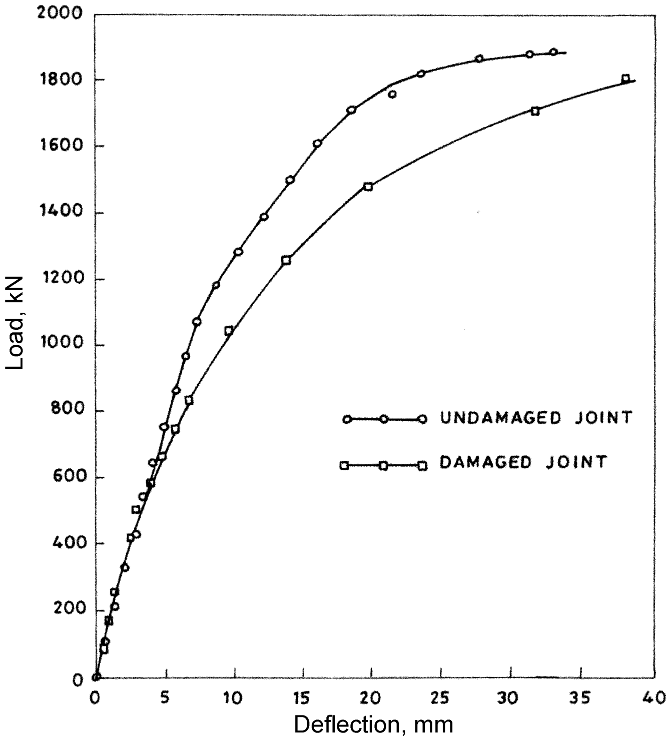

Fig. 12 Load deflection relations of undamaged and damaged joints-typical comparison

In the case of all tested internally ring stiffened Y joints, bending of chord member was observed to be the dominant mode of deformation. In contrast to the case of stiffened T joint, the bending deformation in case of Y joints was mainly due to the component of the load normal to the chord axis because in Y joint the brace is inclined at an angle of 60^o to the chord-axis.

The author had earlier carried out experimental investigation on undamaged internally ring stiffened tubular joints and had published the results elsewhere (Thandavamoorthy 2000). A comparison of typical load-deflection behaviour of an undamaged (Thandavamoorthy 1998) and a fatigue damaged internally ring stiffened tubular T joints has been made in Fig. 12. There is substantial degradation of stiffness of damaged tubular joint when compared to the undamaged joint of the same dimensions. The load corresponding to the initial yielding of the full section of the cracked joint has been reduced to a greater extent, i.e., from a load of 1070 kN for an undamaged joint it has been lowered to 850 kN in the case of the damaged joint. After this load of 850 kN, the damaged joint had undergone a larger deflection under loading. This is due to cracking of the cross section and consequent reduction in stiffness of the joint. As the crack had been formed in some portion of the circumference and had penetrated through the chord wall thickness, the joint seems to rotate about the crack under loading. In all the joints, the circumferential crack widened considerably at ultimate load which seems to be the governing factor for the capacity of the joint.

Typical load-deflection behaviours of the damaged T and Y joints were compared and the same is illustrated in Fig. 13. The behaviours of both the joints were the same upto the yielding of the uncracked full section. After this stage, the T joint, with lesser degree of cracking when compared to the Y joint, has undergone a larger deflection than the Y joint, eventhough the reserve capacity of both the

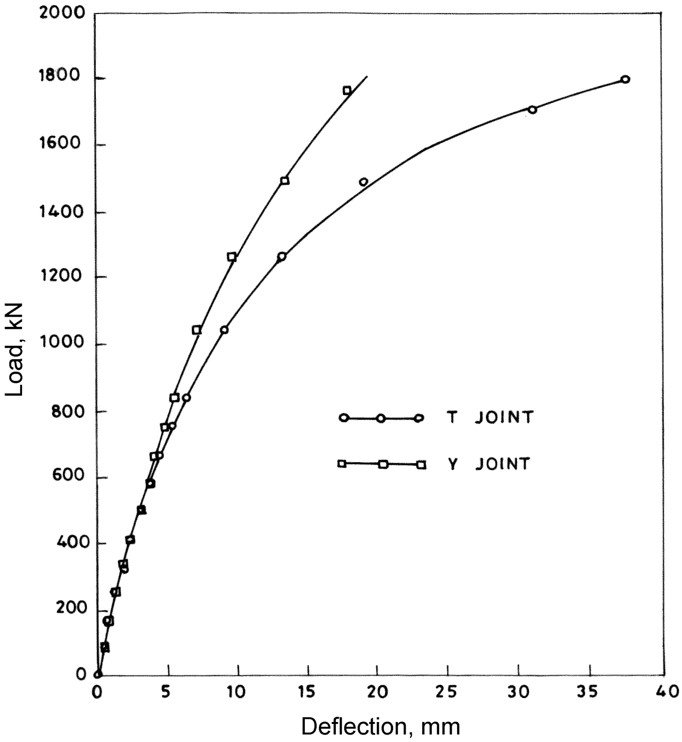

Fig. 13 Comparison of load-deflection relations of fatigue damaged T and Y

joints were almost the same. This is because, in the case of Y joint, the axial component of the load along the chord member stiffens the member considerably with the result the deflection of the joint is reduced to a great extent.

In the case of joint DT1, which was also tested under axial brace tension loading, the initial yielding of the cracked section occurred at 62.5 kN. The uncracked full section yielded at 220 kN. The measured ultimate strength of the joint under tension loading was 400 kN. In this type of loading, the circumferential crack was positioned on the tension side. The area of cross section available for the tensile force is also very small. Therefore there was a drastic reduction in the strength of the joint. Even in axial brace tension loading also, as observed in the case of joint DT1, the predominant deformation of the internally ring stiffened joint was bending only. No ovaling of the chord wall was observed in this case also.

The reduction in strength of the damaged joints under axial brace tension loading is quite substantial as is evident from the residual strength of the joint DT1 tested in tension loading. The capacity of the cracked joint under tension loading is less than one-fourth the capacity of the undamaged joints of the same dimensions under compressive loading. As wave loading falls in the category of reversal of loading, with the presence of such cracked joints in the structure, the tensile nature of the loading may seriously impair the strength of the structure thus jeopardizing its integrity.

5. Conclusions

From the experimental and analytical investigations carried out on corrosion fatigue damaged internally ring stiffened tubular joints, the following conclusions have been drawn.

It was observed in the case of all tested internally ring stiffened fatigue damaged joints that the predominant mode of deformation was bending of the chord member along its longitudinal axis. Absolutely no ovaling and consequent punching of chord occurred in the vicinity of the welded intersection. The distinct advantage of the ring stiffened tubular joint was clearly visible in this experimental investigation. As soon as the cracked section yielded, a re-distribution of load occurred and the uncracked full section was able to carry the load till the ultimate stage. This could be possible only because of the flexural bending of the chord member. Therefore, employment of the internally ring stiffened tubular joints in the construction of offshore structures has the great advantage. Structures provided with internally ring stiffened joints are equipped with necessary in-built load transfer mechanism in the event of being damaged under fatigue loading.

It was observed in this experimental investigation that local bending of the chord wall between the stiffener and the brace face occurred in joints in which the stiffeners were welded away from the brace face. This has affected the load carrying capacity of the joints to some extent. However, no ovaling of chord member occurred. This brings out to the fore, the importance of tolerances and accuracy in welding. Fabrication defects may defeat the purpose for which stiffeners have been welded to the chord wall. This observation assumes significance because such defects may affect the fatigue performance of the structures.

The reduction in strength of the damaged joints under axial brace tension loading is quite substantial. The capacity of the cracked joint under tension loading is less than one-fourth the capacity of the undamaged joints of the same dimensions under compressive loading. Wave loading falls in the category of reversal of loading. With the presence of such cracked joints in the structure, the tensile nature of the loading may seriously impair the strength of the structure thus jeopardizing its integrity.

Experimental investigations carried out on damaged internally ring stiffened tubular joints disclosed that there was substantial degradation of stiffness of the joints vis-à-vis the undamaged joints. The degradation of the stiffness of the damaged joint may lead to large deflection of the structure under loading and perhaps beyond permissible limits too. This may seriously hamper various other functions. The reduction in stiffness of the damaged joint may affect the fundamental frequency of the structure. This may increase the amplitudes of vibration of the structure under wave excitation.

The bi-linear stress-strain model developed for the fatigue damaged internally ring stiffened joints was able to predict their residual strengths fairly close to the experimentally observed values. It has been validated with the experimental results. Equilibrium of forces based on Euler bending theory was first established before the equations necessary to calculate the moment capacity of the damaged joints were derived. This approach is of very general nature and hence the proposed model can be used to assess rationally the residual strength of fatigue damaged internally ring stiffened joints. This model can be incorporated in the codes as design guidelines for the assessment of the residual strengths of fatigue damaged internally ring stiffened tubular joints are hardly available.

References

API RP 2A-LRFD (1993), "Recommended practice for planning, designing, and constructing fixed offshore platforms-load and resistance factor design", American Petroleum Institute, Washington D.C. First Ed., July.

ASTM D 1141-1975 (1980), "Specification for substitute ocean water", *American Society for Testing and Materials*, Philadelphia, Re-approved.

Bian, L.C. and Lim J.K. (2003), "Fatigue strength and stress concentration factors of CHS-to-RHS T-joints", *J. Constr. Steel Res*., **59**(5), May, 627-640.

Bozhen, C. (1990), "Stress analysis of ring stiffened tubular joints for offshore structures - review of studies in China", *China Ocean Engineering*, **4**(1), 1-12.

Calderon, A.S. (2003), "World energy outlook to the year 2020", *Oil Asia Journal*, **24**(1), Jan.-Mar., 8-9.

Cheaitani, M.J. and Burdekin, F.M. (1994), *Tubular Structures VI*, P. Grundy, A. Holgate and B. Wong, (Eds.), A.A. Balkemaa Publisher, Rotterdam, 607-616.

Chen, Y. and Wang, W. (2003), "Flexural behavior and resistance of uni-planar KK and X tubular joints", *Steel and Composite Structures, An Int. J.*, **3**(2), April, 123-140.

Choo, Y.S., Qian, X.D., Liew, J.Y.R. and Wrdenier, J. (2003), "Static strength of thick walled CHS X-joints. Part I. New Approach in Strength Definition", *J. Constr. Steel Res*., **59**(10), October, 1201-1228.

Dexter, E.M. and Lee, M.M.K. (2001), "A general strength prediction formulation for axially loaded planar and multiplanar tubular joints", *Tubular Structures IX,* R. Puthli and S. Herion, Eds., A.A. Balkema Publisher, Lisser, 185-194.

Gowda, S.S. (1991), "Fatigue of steel structures: state of the art", *Proc Fourth Indian Conference on Ocean Engineering*, INCOE-91, N10, Goa, India, 267-274.

IS: 226 (1975), "Indian standard specification for structural steel (standard quality)", Indian Standards Institution, New Delhi, Fifth Revision, April.

Lie, S.T., Chiew, S.P., Lee, C.K. and Huang, Z.W. (2001), "Modelling through thickness and surface cracks in tubular joints", *Tubular Structures IX*, P. Puthli and S. Herion, (eds.), Swets and Zeitlinger, Lisse, 285-290.

Pinna, R., Ronalds, B.F. and Andrich, M.A. (2003), "Cost effective design criteria for Australian monopad platforms", *J. Offshore Mechanics and Arctic Engineering*, ASME, **125**(2), May, 132-138.

Saad, S.B., Leen, S.B, and Hyde, T.H. (2001), "Finite element study on the static strength of a cracked tubular T-joint", *Tubular Structures IX*, R. Puthli, and S. Herion, Eds., A.A. Balkuma Publishers, Lisse, 247-255.

Thandavamoorthy, T.S., Madhava Rao, A.G. and Santhakumar, A.R. (1995a), "Assessment and rehabilitation of damaged offshore structures", *Proc Nordic Steel Construction Conference '95*, Malmo, Sweden Vol. II, 741-747.

Thandavamoorthy, T.S., Madhava Rao, A.G. and Santhakumar, A.R. (1995b), "Damage assessment of offshore structures”, *Structural Steel*, Vol. I Steel Structures, N.E. Shanmugam and V.S. Choo, Eds., Pergamon, Oxford, 551-556.

Thandavamoorthy, T.S., Madhava Rao, A.G. and Santhakumar, A.R. (1998), “Appraisal and repair of damaged steel offshore structures”, *J. the Institution of Engineers (India)*, **78**, February, 147-153.

Thandavamoorthy, T.S. (1998), “Assessment and rehabilitation of damaged offshore structures”, Ph.D. Thesis, Anna University, Chennai, April.

Thandavamoorthy, T.S. (2000), “Investigations on internally ring-stiffened joints of offshore platforms”, *J. Offshore Mechanics and Arctic Engineering*, ASME, **122**(4), November, 233-242.

Thandavamoorthy, T.S. (2002a), “Behaviour of unstiffened tubular joints of offshore platforms”, *J. the Institution of Engineers (India)*, **82**, February, 224-228.

Thandavamoorthy, T.S. (2002b), “Finite element modelling of the behaviour of internally ring stiffened T-joint of offshore platforms,” *J. the Institution of Engineers (India)*, **83**, November, 139-145.

Thandavamoorthy, T.S. (2003), “Comparative behaviour of stiffened and unstiffened welded tubular joints of offshore platforms”, *Steel and Composite Structures, An Int. J.*, **3**(5), October, 321-333.

UEG (1985a), *Design of Tubular Joints for Offshore Structures*, Publication UR 33, Vol. 1, Underwater Engineering Group, London.

UEG (1985b), *Design of Tubular Joints for Offshore Structures*, Publication UR 33, Vol. 2, Underwater Engineering Group, London.

UEG (1985c), *Design of Tubular Joints for Offshore Structures*, Publication UR 33, Vol. 3, Underwater Engineering Group, London.

Valdés V. and Ramirez, R.O. (2000), “Issues and challenges in the requalification of offshore platforms in Mexico”, *J. Offshore Mechanics and Arctic Engineering*, ASME, **122**(3), August, 153-156.

Van Wingerde, A.M., Packer, J.A. and Wardenier, J. (1996), “New guidelines for fatigue design of HSS connections”, *J, Struct, Eng.*, ASCE, **122**(2), 125-132.

CC